Earth Science Faculty Scholarship   Earth Sciences

11-30-1997

Paleoclimatic Variability Inferred from the Spectral Analysis of Greenland and Antarctic Ice-Core Data

R. Yiou

K. Fuher

L. D. Meeker

J. Jouzel

S. Johnsen

See next page for additional authors

Authors

R. Yiou, K. Fuher, L. D. Meeker, J. Jouzel, S. Johnsen, and Paul Andrew Mayewski

Paleoclimatic variability inferred from the spectral analysis of Greenland and Antarctic ice-core data

P. Yiou,[1] K. Fuhrer,[2] L. D. Meeker,[3,4] J. Jouzel,[1]
S. Johnsen,[5,6] and P. A. Mayewski[7]

Abstract. Paleoclimate variations occur at various time scales, between a few centuries for the Heinrich events and several hundreds of millenia for the glacial to interglacial variations. The recent ice cores from Greenland (Greenland Ice Core Project and Greenland Ice Sheet Project 2) and Antarctica (Vostok) span at least one glacial oscillation and provide many opportunities to investigate climate variations with a very fine resolution. The joint study of cores from both hemispheres allows us to distinguish between the sources of variability and helps to propose mechanisms of variations for the different time scales involved. The climate proxies we analyze are inferred from $\delta^{18}O$ and δD for temperature and chemical species (such as calcium) for the joint behavior of the major ions in the atmosphere, which yield an estimate of the polar circulation index. Those data provide time series of climatic variables from which we extract the information on the dynamics of the underlying system. We used several independent spectral analysis techniques, to reduce the possibility of spurious results. Those methods encompass the multitaper spectral analysis, singular-spectrum analysis, maximum entropy method, principal component analysis, minimum bias spectral estimates, and digital filter reconstructions. Our results show some differences between the two hemispheres in the slow variability associated with the astronomical forcing. Common features found in the three ice-core records occur on shorter periods, between 1 and 7 kyr. The Holocene also shows recurrent common patterns between Greenland and Antarctica. We propose and discuss mechanisms to explain such behavior.

1. Introduction

Deep ice-core data provide a mine of information of climate variability over a wide range of time scales, owing to their very fine resolution and their time span. The recent European(Greenland Ice Core Project(GRIP)) and American (Greenland Ice Sheet Project (GISP2)) cores from Greenland and the Vostok core from Antarctica are the longest ice cores, to date, and they all span at least one glacial–interglacial cycle. The GRIP

ice core [*Dansgaard et al.*, 1993] was drilled on the ice divide at Dome Summit (72°34′N, 37°37′W) and reached a depth of 3028 m; the GISP2 site was located 30 km west of GRIP [*Grootes et al.*, 1993] and reached the bedrock at 3053.4 m and penetrated 1.55 m into bedrock. The accumulation rate averages 20 cm/yr; therefore the cores were expected to give detailed information over more than one paleoclimatic cycle, but it is now almost certain that fully reliable time series are limited to the last 110 kyr B.P., the older part being disturbed due to the proximity of the bedrock [*Bender et al.*, 1994; *Chappellaz et al.*, this issue]. The annual cycle can be visually detected on the top parts of the cores, which has therefore an absolute chronology. Annual layer counting was performed on the GISP2 ice core down to ≈ 50 kyr B.P., and the chronology was then established through correlations with the ^{18}O of oxygen in air bubbles between Greenland and other records were performed by *Bender et al.* [1994]; the GISP2 time series in this study use this chronology. The new GISP2 annual layer chronology now extends to 110 kyr B.P. [*Meese et al.*, this issue]. The top 14.5 kyr of the GRIP ice core were also dated by annual layer counting, and the rest of the core was dated with the use of glaciological models [*Dansgaard et al.*, 1993; *Johnsen et al.*,

[1]Laboratoire de Modélisation du Climat et de l'Environnement, Commissariat à l'Energie Atomique, Gif-sur-Yvette, France.

[2]Physikalisches Institut, Universität Bern, Bern, Switzerland.

[3]Department of Mathematics, University of New Hampshire, Durham.

[4]Also at Glacier Research Group and Climate Change Research Center, Institute for the Study of Earth, Ocean, and Space, University of New Hampshire, Durham.

[5]Geophysical Institute, University of Copenhagen, Copenhagen, Denmark.

[6]Science Institute, University of Reykjavik, Reykjavik, Iceland.

[7]Glacier Research Group and Climate Change Research Center, Institute for the Study of Earth, Ocean, and Space, University of New Hampshire, Durham.

1995] . The Vostok project is a cooperative effort between Russia, the United States, and France [*Vostok Project Members*, 1995]; it was drilled in East Antarctica (78°28'S, 106°48'E) and is presently 3125 m deep. The accumulation rate is about 2 cm/yr; this means that the annual layers are too thin for visual detection and models of chronologies have to be used to date the samples [*Lorius et al.*, 1985; *Jouzel et al.*, 1993; *Waelbroeck et al.*, 1995].

From these ice cores, climatic information was retrieved through isotopic measurements of oxygen 18 [*Dansgaard et al.*, 1993; *Grootes et al.*, 1993] and deuterium [*Jouzel et al.*, 1993], greenhouse gases (CO_2 [*Barnola et al.*, 1987] and CH_4 [*Chappellaz et al.*, 1990, 1993]), dust content [*Petit et al.*, 1990], electrical conductivity [*Taylor et al.*, 1993] and various chemical species [*Legrand et al.*, 1992, 1993; *Mayewski et al.*, 1993a, 1993b, 1994, this issue]. We focused on the isotopic measurements ($\delta^{18}O$ and δD), expressed in permil with respect to the standard mean ocean water, and chemical species in the Greenland records. The two isotopes mainly account for the local temperature variations at the top of the inversion layer, where the precipitation formed [*Jouzel and Merlivat*, 1984; *Johnsen et al.*, 1989; *Jouzel et al.*, this issue], while the chemical species are proxies for the intensity of the polar circulation [*Mayewski et al.*, 1993a].

The time series derived from the experimental measurements are generally irregular but bear many resemblances and recurring patterns embedded in noise. These patterns cover the well-documented glacial-interglacial cycle and the abrupt oscillations during the last ice age that are found in all cores. Our challenge is then to decipher the climatic information from these apparently noisy signals and assess the statistical significance of the near periodicities in order to infer plausible physical mechanisms.

Our strategy is to cut our records into identifiable climatic periods. The main reason is that climate dynamics is not necessarily stationary on all time scales. For example, if we look at climatic variations occurring on time scales of centuries to millenia either during an ice age or during an interglacial interval, the two intervals (cold and warm) have very distinct regimes and a global analysis would only average those differences without an appropriate investigation of the proper dynamics of each regime. On the other hand, if we look at slower variations linked to orbital forcing [*Hays et al.*, 1976; *Berger et al.*, 1993], then we obviously need to consider the full length records and the minute temporal details are no longer necessary. Therefore we adapted the time "windows" from the paleoclimatic signals to the processes at play on each characteristic time scale. This methodology is a time–frequency analysis where we have introduced our a priori knowledge of the climatic system.

Massive iceberg discharges from the Laurentide and the Scandinavian Ice Sheets during the last ice age have been documented recently [*Heinrich*, 1988; *Bond and Lotti*, 1995] and generically called "Heinrich events" [*Broecker et al.*, 1992]. They have been associated with sea surface temperature variations over the North Atlantic and temperature variations over Greenland [*Bond et al.*, 1993; *Paillard and Labeyrie*, 1994]. This cumulative evidence points to global climate instability during the last glacial age. This is why we elected to study this particular period of climate history, with its high variability.

The Holocene (11.6 kyr B.P. to present) is the interglacial period we are presently enjoying. Its last 10 kyr have proved to be remarkably stable, compared to glacial-to-interglacial variations [*Johnsen et al.*, 1992]. Fluctuations in the Holocene glaciochemical series, although small compared to those in the glacial portion of the record, reveal marked variability in climate [*O'Brien et al.*, 1996]. Nevertheless, these little variations testify to internal climate variability involving the atmosphere and the ocean during a globally stationary climate and possible (but unknown) solar or volcanic forcings [*Stuiver et al.*, 1995]. Hence we picked this period, in addition to obvious reasons that concern human civilization.

In this paper, we summarize methodological guidelines for time series processing; we particularly insist on the necessity of robust and stable methods, due to the many irregularities in most paleoclimatic signals. These techniques include singular spectrum analysis, the multitaper method, the maximum entropy method, minimum bias spectral estimates, and digital filter reconstructions. Then we apply these recent techniques to the ice-core data described in section 3, for the three climatic periods we described above. The results are given in section 4, where we also propose physical mechanisms to interpret them.

2. Methods

In this section, we describe a few new numerical techniques to extract information from time series. It is important to note that climatological time series very seldom verify the hypotheses required by any mathematical method and that several techniques should be used as cross checks for the validity and stability of results [*Ghil and Yiou*, 1996; *Yiou et al.*, 1995]. Most of the methods here are implemented in a public domain computer tool kit (SSAToolkit) developed by *Dettinger et al.* [1994] (available on the world wide web at http://www.atmos.ucla.edu/). In companion papers [*Mayewski et al.*, this issue; *Meeker et al.*, this issue], alternate techniques, but based on similar principles, are used to extract periodic components. We briefly discuss them in the Appendix.

2.1. Sampling

Data sampling (or resampling) is an important step prior to time series analysis, in the field of paleodata processing. Most signal analysis methods require a reg-

ular time sampling, which is generally not the case for ice-core data. An array of interpolating techniques is described and tested by *Benoist* [1986] and *Yiou et al.* [1995]. It has been shown that the interpolation method of choice can affect the spectral estimates in the high frequencies, hence limiting the relative confidence in this part of the spectrum [*Yiou et al.*, 1995]; overall, however, less than one third of the frequency range seemed affected by the choice of the interpolating method.

The technique we adopted proceeds by averaging the signal over nonoverlapping "bins" of equal time intervals τ [*Benoist*, 1986; *Yiou et al.*, 1995]. This scheme corresponds to a weak low-pass filter [*Benoist*, 1986]. The property of this interpolation process is that the Nyquist period is 2τ. If the intrinsic process does not contain power in the $[-1/\tau, 1/\tau]$ frequency band, then the aliasing is negligible with this interpolating scheme. Numerical experiments [*Yiou et al.*, 1995] show that it does not create spurious oscillations (contrary to regular cubic spline methods) and hence the spectrum can be estimated with more confidence. On the other hand, this method is only useful when one is willing to undersample the time series, i.e., if τ is greater than a typical time step of the signal. If oversampling is desired, another type of interpolation, using the physical relation linking depth and time in order to preserve the data skewness, can be used, with little spectral alterations.

2.2. Singular Spectrum Analysis

Singular spectrum analysis (SSA) is designed to extract information from short and noisy time series and give hints on the (unknown) dynamics of the underlying system that generated the series [*Broomhead and King*, 1986; *Vautard and Ghil*, 1989]. It was motivated by mathematical and experimental results [*Takens*, 1981; *Packard et al.*, 1980], which showed that under generic conditions, a time series of observables from a dynamical system contains enough information to reconstruct this "unknown" dynamical system. The starting point of the method is to embed a time series $\{X(t)\}$, $t = 1, \ldots, N$ in a vector space of dimension M, with M presumably larger than the effective but unknown dimension d of the underlying system. The embedding procedure constructs a sequence $\{\tilde{X}(t)\}$ of M-dimensional vectors of delayed coordinates from the time series X:

$$\tilde{X}(t) = [X(t), X(t+1), \ldots, X(t+M-1)], \quad (1)$$

with $t = 1, \ldots, N - M + 1$. If d is larger than four or the time series contains (random) noise, a raw application of this technique will fill any two-dimensional projection in a dense way so that no information can be retrieved. SSA allows us to unravel the information entangled in the delayed coordinate phase space by decomposing the constructed sequence of vectors into elementary oscillation patterns. Hence this method generates data-adaptative filters for the separation of the time series into statistically independent components, like trend, deterministic oscillations, and noise. Thus a clean signal can be analyzed through reconstructed components (RCs), pattern-wise or by using other mathematical tools [*Allen*, 1992; *Vautard et al.*, 1992]. Details of SSA algorithms and properties have been investigated by *Penland et al.* [1991], *Vautard et al.* [1992], and *Allen* [1992].

An important step in signal processing (and SSA in particular) is the quantitative detection of noise and its characteristics. Climatic time series are often contaminated by red noise, which affects preferably low frequencies; it is a first order autoregressive process whose spectral characteristics ($\approx 1/f^2$ shape in a frequency diagram) are generic in climate time series [*Ghil and Childress*, 1987; *Allen*, 1992]. In general, very crude tests can be devised from comparisons with an "idealized" noise process: the spectrum of a noise process is known to have a particular shape, and if the data spectrum lies above an ideal noise spectrum, it is generally considered as "significant." This approach can be very deceptive because a single noise realization can have a very different spectrum from an ideal one, especially if the number of data points is small; it is the average of such spectra over many realizations that will tend to the spectrum of the ideal noise process. *Allen* [1992] devised tests to compare the statistics of simulated (or surrogate) red noise time series with those of a climatic signal; this is the Monte Carlo SSA (MC-SSA). Alternatives to MC-SSA, based on a standard procedure of principal component analysis [*Preisendorfer*, 1988] to estimate distributions of serial correlations, can also be used with a smaller computing cost [*Lall and Mann*, 1995]. Multivariate generalizations of (MC-) SSA have been developed by *Plaut and Vautard* [1994] and *Allen and Robertson* [1996].

2.3. Multitaper Method

The purpose of this nonparametric spectral method [*Thomson*, 1982; *Percival and Walden*, 1993] is to circumvent the problem of the variance of spectral estimates; indeed, the variance of raw Fourier spectrum of a random process equals the spectrum itself [*Jenkins and Watts*, 1968], which means that the potential errors can be as large as the calculation itself. A set of independent estimates of the power spectrum is computed, by premultiplying the data by K orthogonal tapers, i.e., functions which are built to minimize the spectral leakage outside a scaled bandwidth $N\Omega$ (Ω is a frequency bandwidth) due to the finiteness (N) of the data. Then, averaging over this ensemble of spectra yields a better and more stable (with lower variance) estimate than with single-taper methods [*Thomson*, 1990]. Detailed algorithms for the calculation of those tapers are given by in *Thomson* [1990], *Percival and Walden* [1993], and *Rögnvaldsson* [1993]. The choice of K and $N\Omega$ is a trade-off between stability and frequency resolution, so that several values should be tested [*Yiou et al.*, 1996].

Harmonic analysis (estimate of line frequencies and their amplitude) can be performed by MTM, with a statistical F test on the amplitude. One of the main assumptions of MTM harmonic analysis is that the signal must yield periodic and separated components. If not, a continuous spectrum (from a colored noise or a chaotic system) will be broken down to spurious lines with arbitrary frequencies and possibly high F values. This is a danger of the method, which can be partially avoided if the raw power spectrum is computed, hints for lines are detected, and the parameters $N\Omega$ and K are varied.

Time-frequency analyses (evolutive spectral analyses) with moving windows were performed with this method by *Yiou et al.* [1991] and *Birchfield and Ghil* [1993]. In addition, a multichannel MTM generalization (i.e., with a spatial extent) has been investigated by *Mann et al.* [1995].

2.4. Maximum Entropy Method

The maximum entropy method (MEM) is potent to estimate line frequencies in an autoregressive time series. Exhaustive details are given by *Burg* [1967] or *Childers* [1978].

MEM is very efficient for detecting frequency lines for stationary time series. If this hypothesis is not verified, or if the time series is not close to autoregressive, cross testing the time series with other techniques is necessary. Moreover, the behavior of the spectral estimate depends on the choice of the autoregression order M: the number of peaks in the spectrum increases with M, regardless of the time series content. An upper bound for M is generally taken as $N/2$. Heuristic criteria have been devised to refine the choice of a reasonable M [*Haykin and Kessler*, 1983; *Benoist*, 1986], based on a minimization of the residual of a least squares fit between the autoregressive approximation and the original time series [*Haykin and Kessler*, 1983]. The use of such criteria can be tricky because they all appear to underestimate the order of regression of a time series [*Benoist*, 1986]. Thus they still do require trial-and-error sensitivity tests [*Yiou et al.*, 1996].

2.5. Empirical Orthogonal Function Analysis

Empirical orthogonal function (EOF) analysis [*Peixoto and Oort*, 1992], like principal component analysis (PCA) [*Peisendorfer*, 1988], is used for multivariate data in the hope that a new basis can be found so that the information in the data is expressed with fewer coordinates. Its formulation is quite similar to the SSA method and it is useful for data with more than two variables. In principle, SSA theory can be embedded into PCA, as the computations essentially involve the diagonalization of a covariance matrix and projections onto the eigenvectors. We exposed at length SSA in this paper, thus we will be very brief for PCA, which is used to extract a common variation component within a set of chemical measurements.

In practice, we have a sequence of vectors V_n, $n = 1, \ldots, N$, e.g., eight-dimensional vectors representing the variations of chemical species measured in the GISP2 ice core [*Mayewski et al.*, 1994]. Then we want to compute a basis in this multi dimensional space (eight-dimensional in this particular case), in which the variance is most efficiently represented; that is, it can be described by the least possible number of vectors. If V denotes the $N \times M$ matrix containing the sequence of N data M-dimensional vectors V_n, then the covariance C of the matrix V is

$$R = \frac{1}{N}CC^t, \qquad (2)$$

where the superscript t denotes matrix transposition. We then look for the eigenelements of the symmetric and definite positive matrix R by solving

$$Re_k = \lambda_k e_k, \qquad (3)$$

where the M vectors e_k are called the EOFs, as with SSA. Projections P_k of the data V onto this eigenbasis can be defined as

$$P_k = e_k^t V. \qquad (4)$$

They give a new representation of the data in which each P_k represents $\lambda_k/\lambda_1 + \cdots + \lambda_M$ percent of the covariance of V.

For example, the first and the second EOF in the GISP2 chemical species record represent 70% and 14%, respectively, of the variance of the data.

3. Data

As explained in the introduction, we focused on two types of data with a very high temporal resolution: isotopes and chemical species. The GISP2 chronology we use is based on annual layer counting down to ≈ 50 kyr and then derived by correlations with ^{18}O of O_2 [*Bender et al.*, 1994]. For the GRIP ice core, the chronology was based on layer counting down to 40 kyr; the rest of the core was dated with a glaciological model [*Dansgaard et al.*, 1993] and correlation with a marine-sediment record [*Grootes et al.*, 1993].

The Vostok records were dated using a glaciological model [*Jouzel et al.*, 1993] with a control point at 110 kyr B.P., where the record is assumed to be synchronous with the Spectral and Mapping Project (SPECMAP) record at marine stage 5 [*Jouzel et al.*, 1993]. Alternative chronologies based on correlation with deep-sea core records [*Sowers et al.*, 1993] or orbital tuning [*Waelbroeck et al.*, 1995] have also been explored.

3.1. Isotopes

We studied oxygen 18 (GRIP/GISP2) and deuterium (Vostok) from the core water. Those values are normalized to standard mean ocean water (SMOW) and expressed in per mil delta values. These isotopes are proxies for the temperature of formation of the precip-

itation (at the inversion layer) as shown by numerical [*Jouzel and Merlivat*, 1984; *Jouzel et al.*, 1994] and experimental studies [*Johnsen et al.*, 1989]. *Jouzel et al.* [this issue] review the assessment of the temperature–isotope relationship. The relationship between the isotopic content of snow and temperature at the precipitation site has been investigated for Greenland through observations of present-day distribution in surface snow [*Johnsen et al.*, 1989] and examined through a hierarchy of isotopic models [*Jouzel et al.*, this issue and references therein]. The use of present-day spatial temperature–isotope gradient for interpreting the Greenland isotopic profiles has been challenged by recent paleothermometry measurements [*Cuffey et al.*, 1995; *Johnsen et al.*, 1995b]. Those two studies led to the conclusion that the isotopic ratios can be used as paleothermometers, and each group has, using different calibration procedures, produced a central Greenland temperature record. We have based our spectral analyses on the isotopic records themselves and checked that the spectral properties are not significantly modified when the temperature records inferred either from the present-day isotope relationship (throughout the records as currently done at Vostok) or time dependent calibration [*Cuffey et al.*, 1995; *Johnsen et al.*, 1995b] are used.

The sampling for all the cores is continuous and detailed: 55 cm, 1 m at GISP2, and either 50 cm or 1 m at Vostok (with few 2-m samples). Therefore the time sampling varies from a few years (the upper part of the Greenland cores) to 100 years, with larger sampling intervals (up to 200 years) for the periods near 50, 60, and 100 kyr B.P. at GRIP, GISP2, and Vostok, respectively. Therefore we generated several time series with different time steps (and the interpolating technique described above) from each record, depending on the length of the records (full record, glacial period, or Holocene) and the time scale to be investigated. The full-extent isotopic profiles for the three cores are shown in Figure 1.

3.2. Soluble Ions

Soluble ions (Ca, Na, Cl, SO$_4$, K, Mg, NH$_4$, and NO$_3$) were measured at a resolution of 0.6–2.5 years through the Holocene, a mean of 3.48 years through the deglaciation, ≈ 3–116 years throughout the remainder of the 110,000-year long portion of the record, and at lower resolution over the rest of the core, for a total of 16,395 samples [*Mayewski et al.*, 1990b, 1993a, 1993b, 1994, this issue; *Fuhrer et al.*, 1993]. The sources for the chemical species transported to Greenland are primarily terrestrial dust and marine surfaces [*Mayewski et al.*, 1990a]. It was suggested that changes in atmospheric composition could be accounted for by changes in the size of the polar atmospheric cell, resultant changes in source regions and the modifications of continental biogenic source regions [*Mayewski et al.*, 1993a, 1993b, 1994]. Similarly, *Alley et al.* [1996] used a simple model to show that the chemical concentrations (in the GISP2
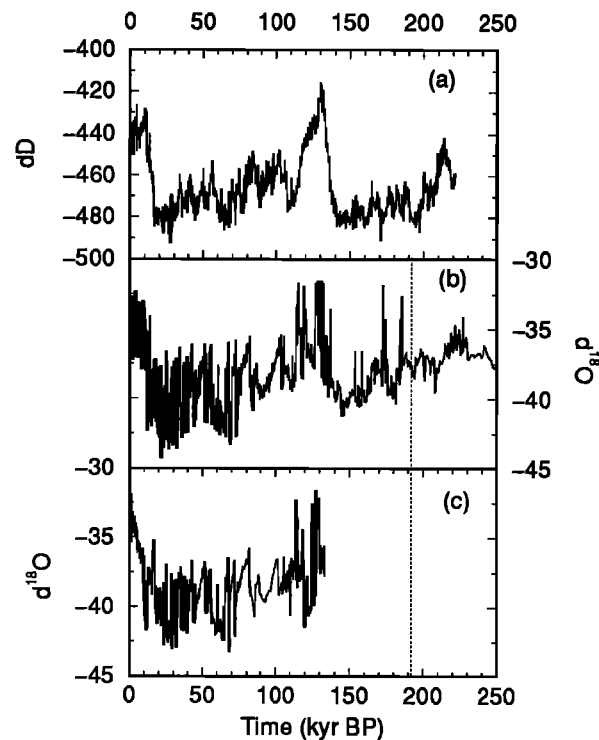

Figure 1. Isotopic variations in the (a) Vostok, (b) GRIP and (c) GISP2 ice cores. The profiles are expressed in per mil versus SMOW; time goes from the right to the left and is expressed in kiloyears B.P. Figure 1a shows deuterium content, and Figures 1b and 1c show oxygen 18 content. The vertical dotted bar in the Greenland ice-core profiles indicates the time restriction we took (110 kyr B.P.) for our spectral analyses.

snow and ice) follow atmospheric fluxes and hence provide a history of atmospheric circulation [*Mayewski et al.*, this issue].

The GISP2 ion measurements were grouped by a principal component analysis, as described previously in order to highlight their similitudes and differences. This allowed us to create robust composite variables of the climate system, by identifying strong and recurrent patterns of oscillations. The average time sampling is very fine, but we subsampled the data to a time interval of $\tau = 200$ years to make comparisons with isotopic data possible.

The ion concentrations are all positive with a strong asymmetry toward large values. Hence we normalized them through their logarithm in order to preserve stationarity and symmetry between lower and higher values. Indeed, noise tests generally assume that the processes are at least pseudo-Gaussian, which would not be the case if the raw data were used. Spurious harmonics can also be introduced if a Fourier analysis is performed. It turns out that our results are only marginally affected when replacing the raw unnormalized data.

We plotted the temporal variations during the last ice age of Ca (GRIP [*Fuhrer et al.*, 1993]) on a logarithmic scale (Figure 2b). These variations are strikingly similar
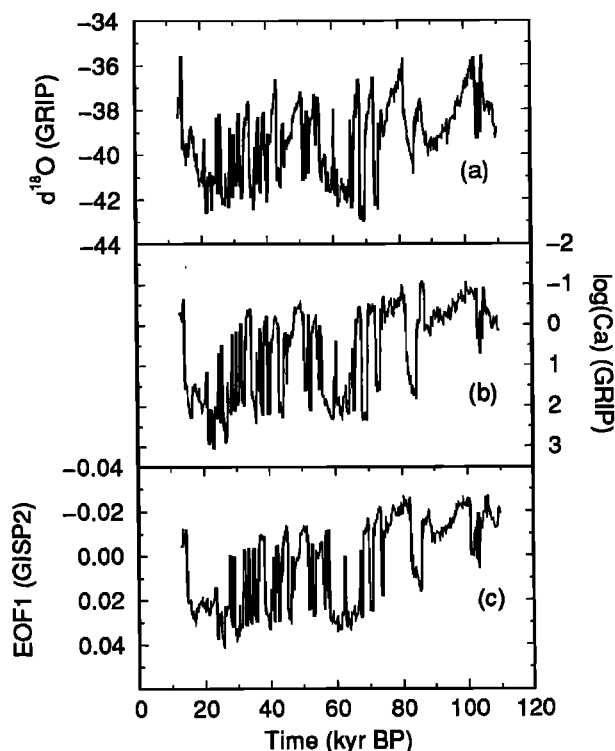
Figure 2. (a) For comparison purposes the $\delta^{18}O$ profile at GRIP during the last ice age is plotted. (b) The log-transformed calcium variations during the last ice age at GRIP. (c) The EOF1 variations of eight chemical species measured at GISP2 are shown. Time axis and units are as in Figure 1.

(in fact, anticorrelated) to the $\delta^{18}O$ values at GRIP (Figure 2a), with a high correlation coefficient, $r^2 = 0.79$; the linear regression relation

$$\delta^{18}O = -38.42 - 1.38\log(Ca),\qquad(5)$$

exhibits fairly low dispersion (Figure 3a). This means that calcium values are high during interstadials (cold periods, with low $\delta^{18}O$). Surprisingly, it turns out that this dispersion is close to the one in $\delta^{18}O$-temperature relations. We notice that the calcium–oxygen 18 relationship during the last glacial period is divided into two clusters with different slopes. This suggests the existence of two dynamical atmospheric regimes in the glacial climate, during stadials and interstadials; they are linked to the nonlinear saturation of climate instabilities on this time scale [Ghil et al., 1991].

To first order, $\delta^{18}O$ and chemical species seem to be driven in the same way by local (northern high latitude) climate changes. The residual $r_c = \delta^{18}O - a\log(Ca) - b$, with $a = -1.38$ and $b = -38.42$, would then account for processes that are not governed by local temperature, like processes occurring or driven at low latitudes. The variations of r_c are plotted in Figure 3b.

On the other hand, the first EOF of the chemical species assemblage from the GISP2 ice core [Mayewski et al., 1994], plotted in Figure 2c, has a much smaller

correlation coefficient with the $\delta^{18}O$ record at GISP2 or GRIP ($r^2 = 0.25$, not shown): there seems to be a first-order linear relationship comparable with that of Ca at GRIP, but the dispersion is much higher. Therefore we did not create a composite residual variable from this EOF and an isotopic record.

4. Results

We focused on three characteristic time scales relevant to paleoclimate variations. This circumvents the possibility of nonstationarity of the records (and the system itself) because it is very likely that the climate system wanders through different states (even during an ice age) for which only local stationarity can be assumed [Imbrie et al., 1992].

4.1. Glacial–Interglacial Oscillation

The study of the full-extent records was done to circumscribe the role of the astronomical forcing on long time scales. This role has already been documented extensively, in marine cores (Crowley and North [1991] give many examples) and in ice cores [Benoist, 1986;
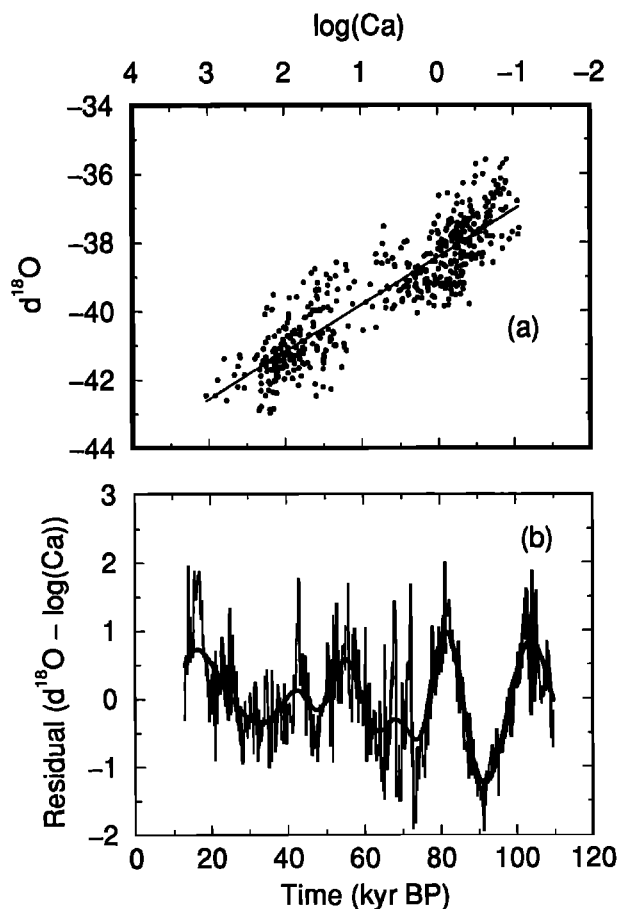

Figure 3. (a) The linear regression between $\delta^{18}O$ and log(Ca). (b) Plot of the residual r_c, expressed in $\delta^{18}O$ per mil, from the linear regression from Figure 2c (thin line). The thick line is the reconstruction of SSA principal components 1 and 2, which account for the slowly varying components of r_c.

Jouzel et al., 1987; *Johnsen et al.*, 1995a; *Waelbroeck et al.*, 1995], with various techniques. We concentrated on isotopic records from the Vostok (δD) and the two Greenland cores (δ^{18}O), which span a complete glacial–interglacial cycle and include an excellent resolution for the Holocene. We sampled the data with an average step of $\tau = 0.5$ kyr. MTM analyses show that low-frequency components close to the Milankovitch frequencies (obliquity, 41 kyr; precession of equinoxes, 23 kyr and 19 kyr) are present in all records. The very low frequency component, associated with the full glacial–interglacial oscillation, can hardly be interpreted based on eccentrity forcing, because it is observed at most twice in the Vostok record and only once in the Greenland cores. An obliquity component (around 41 kyr) appears in Figure 4 in the Vostok ice core (dated from the extended glaciological timescale [*Jouzel et al.*, 1993]) and in the Greenland records (in Figure 5, and shown by *Mayewski et al.* [this issue]). This component is more stable in the Vostok isotopic signal than in the Greenland signals, possibly due to the different lengths of the records or the different chronologies. On the other hand, precessional components (around 23 kyr) appear to be more stable and with a larger relative amplitude (with respect to MTM parameter changes) in the Greenland records than in the Vostok one.

An important caveat of this analysis is that it cannot be confirmed by MEM because it requires very large autoregressive orders (which are several times larger than the one preconized by standard tests [*Haykin and Kessler*, 1983]) in order to find Milankovitch frequencies. MC-SSA is not sensitive enough to assess the presence (or absence) of such slow variability.

The slight discrepancy between the two hemispheres can have essentially two origins. The first is rather technical and would be errors in the chronologies of one or all the records. The chronologies are trusted to have 10% error bars in age, but local perturbations of such amplitude can induce changes in the low-frequency
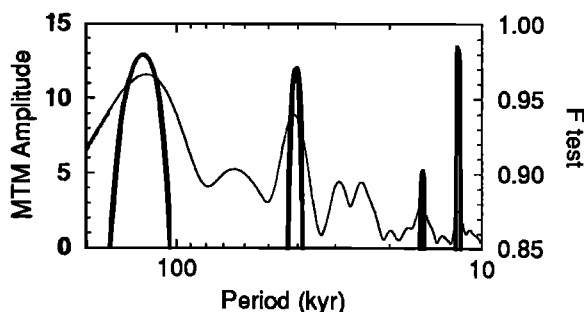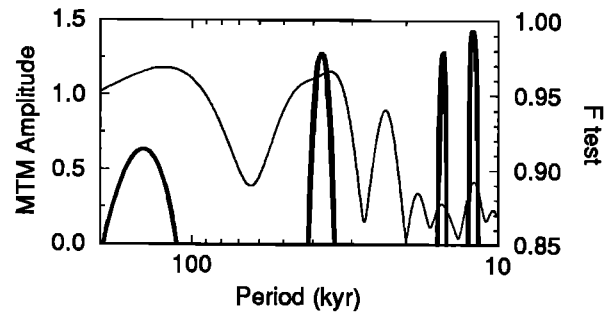

Figure 5. MTM harmonic analysis of the GRIP oxygen 18 record. The MTM parameters and axis captions are the same as in Figure 4.

spectra. Experiments with different chronologies for the Vostok deuterium record have been performed [*Waelbroeck et al.*, 1995] but they were based on orbital tuning [*Martinson et al.*, 1987] of the chronology, for which the identification of Milankovitch frequencies can be biased because they are deliberately introduced into the signal. On the other hand, if the chronologies are (provisionally) trusted not to alter the spectra in the low-frequency band (and this is a bold assumption), then climatological explanations can be attempted: the precessional forcing affects most strongly the Asian monsoon [*Kutzbach and Otto-Bliesner*, 1982; *Kutzbach and Guetter*, 1984]. This is coupled to the Arctic, but not to the Antarctic circumpolar circulation, via the flow over Tibet and Siberia [*Marcus et al.*, 1994, 1996]. An alternate explanation is that the Antarctic circumpolar vortex reduces the influence of the meridional transport from the low latitudes to Antarctica, hence altering its precessional component which is mostly found in equatorial and tropical latitudes [*Crowley and North*, 1991; *Imbrie et al.*, 1992].

4.2. Glacial Period

We took the deuterium profile at Vostok and the oxygen 18 and (previously defined) Ca residual records in GRIP/GISP2 to study the glacial period (110 to 13 kyr B.P.). The records were sampled every 200 years. The general shape of the MTM and MEM spectra is akin to that of red noise, with a few frequency bumps (Figure 6).

From a MC-SSA analysis, the Vostok record contains components with periodicities near 37 and 18 kyr which can be attributed to obliquity and precessional changes (Figure 6c). These periodicities are also detected by MTM (Figure 6a), but not with MEM, using a moderate autoregression order ($M = 20$, Figure 6b). The higher frequencies contain significant components around 10 and 6 kyr. The former could be a precessional harmonic [*Yiou et al.*, 1991; *Hagelberg et al.*, 1994], but the 6 kyr near cycle is close to the behavior predicted by simple ice sheet oscillation models [*Ghil and Le Treut*, 1981; *MacAyeal*, 1993]. From these results only, we cannot identify which ice sheet (Antarctica or northern
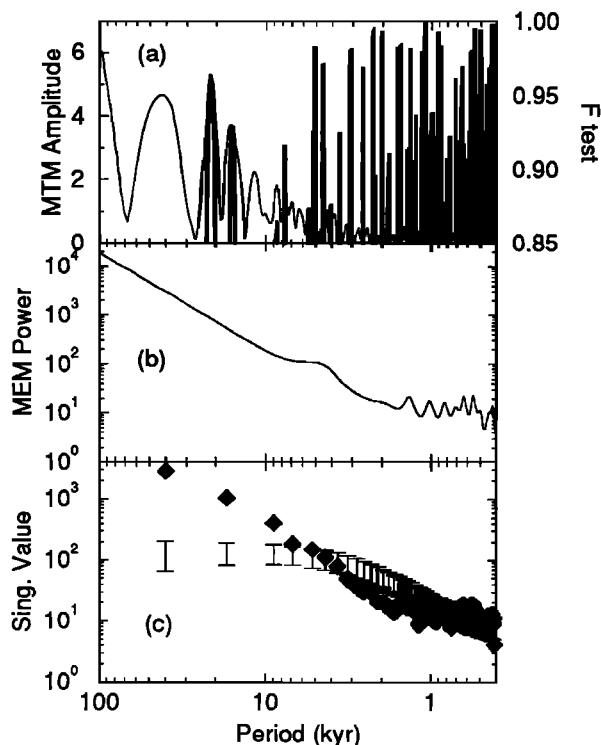

Figure 4. MTM harmonic analysis of the Vostok deuterium record. The parameter values are $N\Omega = 2$ and $K = 3$ tapers. The horizontal axis represents period (in kiloyears), the left axis is estimated amplitude (light solid line) and the right axis is the statistical F test (heavy solid line).

Figure 6. Spectral analyses of the glacial Vostok deuterium record. (a) A MTM harmonic analysis ($N\Omega = 4$ and $K = 7$); left and right axis as in Figures 4 and 5. The logarithmic horizontal axis is period, expressed in kiloyears. (b) A MEM spectrum ($M = 20$). (c) A Monte Carlo SSA analysis, with a window width of $M = 60$. The error bars give the 90% red noise percentiles: the diamonds falling between the bars correspond to signal components which are 90% indistinguishable from red noise.

same spectra (not shown) as the isotopic record, and the behavior of the EOF1 at GISP2 was investigated by *Mayewski et al.* [1993, 1994] who found similar results. But the records seem to contain slightly faster millenial components, with periods between 4 and 5 kyr (Figure 7). This type of behavior has already been associated with the massive iceberg discharges from the Laurentide Ice Sheet into the North Atlantic [*Bond et al.*, 1993; *Yiou et al.*, 1994]. These discharges are not exactly periodic (in a strict mathematical sense), and other Northern Hemisphere ice sheets can discharge icebergs too [*Bond and Lotti*, 1995]; therefore it is anticipated that what is observed through spectral analysis is an average periodicity of such a phenomenon. Yet, the timing of Heinrich events can be approximated by an $\approx$ 6-kyr band-pass component in the glaciochemical time series [*Mayewski et al.*, this issue].

A comparable resolution in both cores allows us to investigate the connection between the almost cyclical features in the Greenland and Antarctic cores. *Bender et al.* [1994] have put the GISP2 and the Vostok isotopic records on a common timescale, through $\delta^{18}O$ content in air bubbles, and found that each interstadial in Vostok coincides with a long interstadial in GISP2. Such a synchroneity on this time scale would imply a global oscillating mechanism whose response time involves at least one ice sheet instability; the Laurentide ice sheet is then a good candidate to drive such variability. *Bender et al.* [1994] argue that the connection to the southern hemisphere can go through the thermohaline cir-
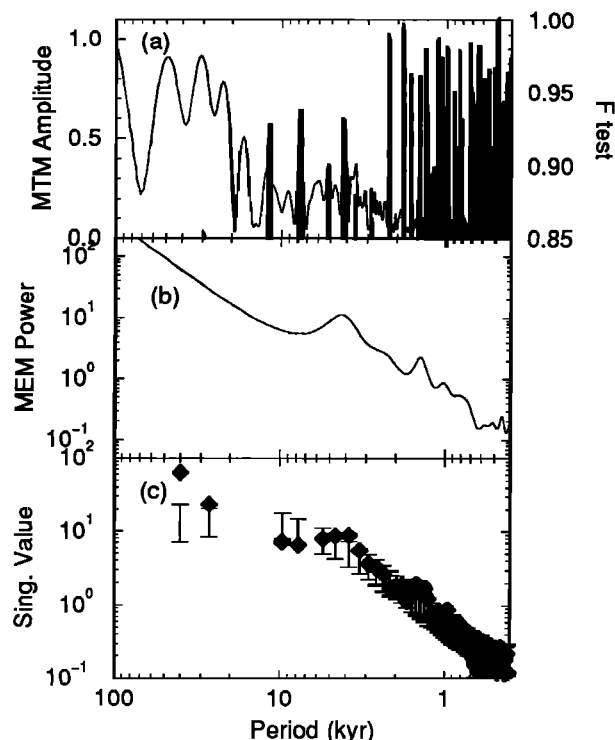
hemisphere ice sheets) is susceptible to provoking such oscillations, but evidences of iceberg discharges around West Antarctica [*Shemesh et al.*, 1994] could give such an explanation. A reconstruction associated with this component reveals variations close in amplitude to the largest fluctuations observed in the raw data during the glacial period, as already shown by *Yiou et al.* [1994].

The rest of the spectrum is either statistically indistinguishable from red noise or has very low amplitude peaks that cannot be interpreted in simple physical terms. We performed similar analyses on time series based on a chronology obtained with correlation with SPECMAP data through $\delta^{18}O$ in O_2 [*Sowers et al.*, 1993]. This correlation, which roughly corresponds to a compression of the chronology during the last ice age, reduces to $\approx$ 4 kyr the periodicity of the oscillation we detected in Figure 6 with the timescale of *Jouzel et al.* [1993]. This result (not shown) is not very surprising, and it allows us to give an interval for the average periodicity of this oscillation.

The Greenland $\delta^{18}O$ records have a similar behavior in the low-frequency band, as noticed by *Yiou et al.* [1995]. The ion concentration records yield the

Figure 7. Spectral analyses of the glacial GRIP oxygen 18 record (the GISP2 record gives identical results). Same panels and parameters as in Figure 6.

culation, as modeled by *Ghil et al.* [1987]. Indeed, modifications in the rate at which North Atlantic Deep Water (NADW) sinks and flows southward has implications on the southern hemisphere heat budget and hence temperature. On the other hand, with the "common" time frame of *Bender et al.* [1994], the Vostok record sometimes leads the GISP2 record by 1 or 2 kyr, and the Greenland ice cores yield a larger number interstadials. We propose to reconcile this slight discrepancy with possible instabilities of the West Antarctic Ice Sheet and the occurrence of iceberg discharges into the Southern Ocean: such events, described by *Shemesh et al.* [1994], could in turn affect the northern hemisphere through the ocean circulation or ocean level. A theory for such a global ice sheet instability scenario, with several ice sheet oscillators, has also been proposed by *Yiou et al.* [1995] and *Verbitsky and Saltzman* [1994, 1995].

In the very high frequency domain, we also note the presence of a significant, almost periodic component around 1.5 kyr, which was also found in high-resolution North Atlantic marine records [*Stocker and Mysak*, 1992; *Cortijo et al.*, 1995]. It is even stronger in EOF1 of the GISP2 chemical species. This component could be attributed to the variability of the oceanic thermohaline circulation [*Weaver et al.*, 1993; *Quon and Ghil*, 1995]. Long-term simulations of coupled ocean–atmosphere models should assess this component.

The chemical species residue r_c at GRIP shows a prominent precessional component (Figures 8a,c) sim-
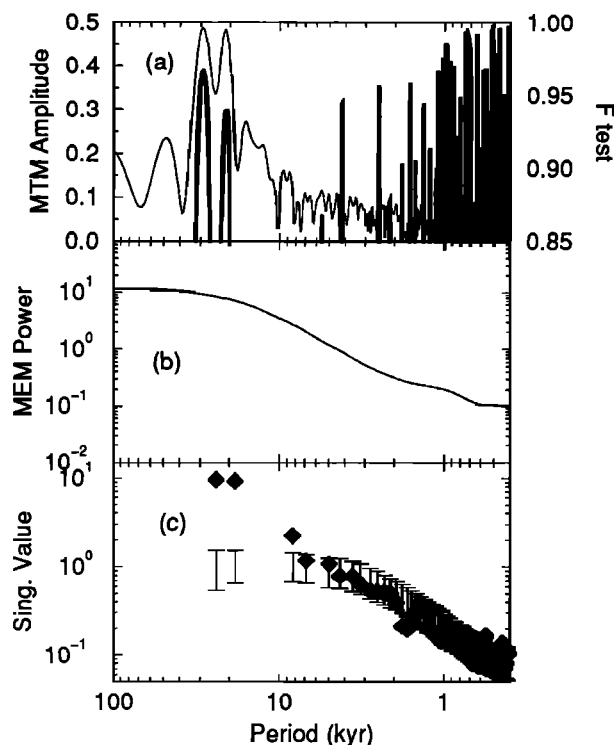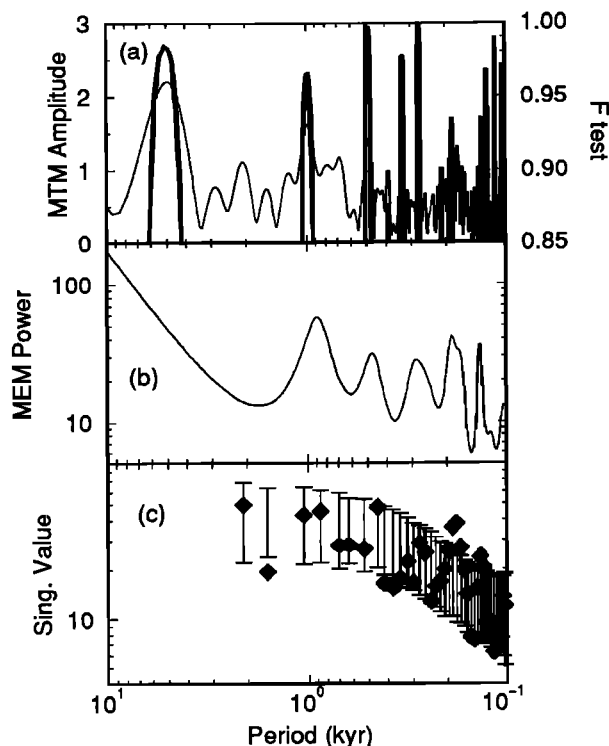

Figure 9. Spectral analyses of the last 10 kyr of the Holocene deuterium record at Vostok. Panels are the same as in Figures 6–8; the parameters are $N\Omega = 6$ and $K = 8$ in Figure 9a, $M = 20$ in Figure 9b and $M = 40$ in Figure 9c.

Figure 8. Spectral analyses of the glacial GRIP oxygen 18 residual r_c record. Same panels and parameters as in Figure 6.

ilar to that found in the GISP2 ammonium series derived from mid-low latitude continental biogenic sources [*Meeker et al.*, this issue]. We reconstructed this precessional component with the SSA algorithm [*Vautard et al.*, 1992], with the first two EOFs, and plotted this reconstruction in Figure 3. Apart from a periodicity at 9.8 kyr (close to a harmonic of a precessional cycle), the faster variations are within the red noise statistics (Figure 8). In particular, no fast variations related to Heinrich events are detected in this "residual" record. This precessional component shows that the nonlocal climate variability (i.e., over source regions) of $\delta^{18}O$ comes from low latitudes which show larger precessional components [*Crowley and North*, 1991]. Therefore it seems possible to retrieve low-latitude climatic information from a heterogeneous couple of time series at the same location.

4.3. Holocene

The Holocene period (11.6 kyr B.P. to present) was analyzed on the isotopic series from the Vostok (Figure 9) and GRIP (Figure 10) records. The time sampling was taken as $\tau = 50$ years. MTM spectra and a noise test with Monte Carlo SSA (Figures 9c and 10c) show that most of the records are indistinguishable from red noise over most of the frequency range from 1/100 to 1/10000 years^{-1}. In the GRIP record, a few fast components stand out above a nineteenth percentile of this
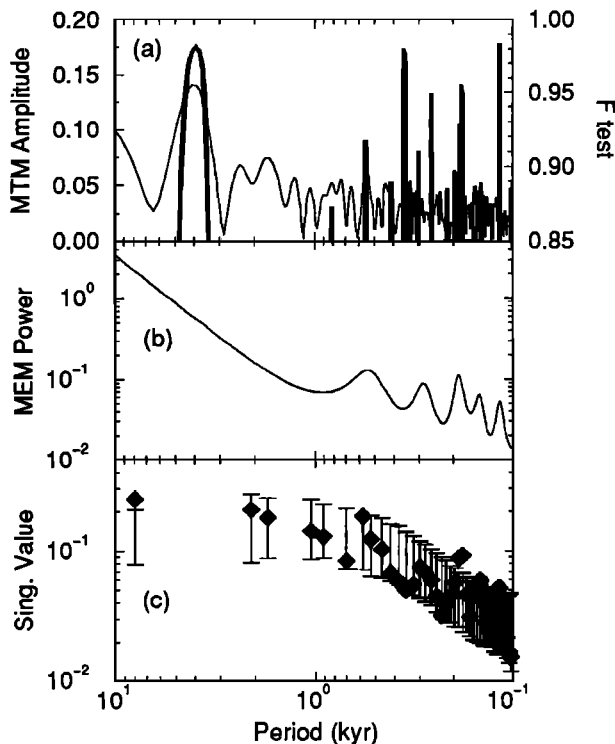
Figure 10. Spectral analyses of the Holocene GRIP oxygen 18 record. Same panels and parameters as in Figure 9.

noise background (Figure 10c) at periodicities around 2 kyr, 180 years, 150 years and 120 years. These periodicities are also found by MTM harmonic analysis and MEM (Figures 10a and 10b). They are robust to parameter changes; hence this stability between independent techniques strongly enhances the confidence of these peaks. The Holocene period in the deuterium profile at Vostok shows similarities with the GRIP record, with significant components detected by MC-SSA near 180 and 130 years standing out above the red noise spectrum. We notice that both MTM and MEM can give spurious peaks when compared with MC-SSA. This is due to the fact that both of the former methods tend to break broadband noise into discrete lines (MTM) or sharp peaks (MEM).

The significant oscillations occur during a relatively ice sheet free period (the Holocene), hence they are less likely to be associated with glacial events or major ice sheet (recurring) oscillations. External (e.g., astronomical or solar) forcings can play a role on these time scales [*Stuiver et al.*, 1995], even though the physical mechanisms, the energy variations are very small, relating solar constant fluctuations to such climate variations are not yet documented. On the other hand, this type of centennial-to-millenial oscillations starts to be documented in other high-resolution data [*Stocker and Mysak*, 1992; *Mann et al.*, 1995] and models of the general circulation of the ocean, either uncoupled [*Weaver and Hughes*, 1994; *Chen and Ghil*, 1995] or coupled with a sea ice [*Yang and Neelin*, 1993] or an atmospheric

[*Delworth et al.*, 1993; *Chen and Ghil*, 1996] model, are simulating such oscillations that seem to arise from instabilities of the thermohaline circulation.

5. Conclusions

In this paper we have applied advanced techniques for time series analysis encompassing singular spectrum analysis, multitaper method and maximum entropy method. These techniques allowed us to disentangle, to some extent, the complex paleoclimatic information contained in Greenland and Antarctic ice-core signals through oscillation detection. We have highlighted the presence of slow components close to the orbital frequencies, which agree with the ideas on the role of astronomical forcing in of paleoclimate [*Berger et al.*, 1993]. The greater strength of the precessional component in Greenland might be due to the stronger coupling between the monsoonal circulation [*Kutzbach and Otto-Bliesner*, 1982; *Kutzbach and Guetter*, 1984] and the northern high latitudes.

During the last ice age, the isotopic records exhibit rapid variability with periodicities between 4 and 7 kyr. This type of behavior can be explained by ice sheet/climate interactions [*Ghil and Le Treut*, 1981; *MacAyeal*, 1993], as supported by the fact that iceberg discharges correlate very well with this fast isotopic variation in both hemispheres [*Bond et al.*, 1993]. Therefore the cyclical pattern we found in the isotopic data can be attributed to such a mechanism. *Shemesh et al.* [1994] have shown evidence for iceberg discharges into the Antarctic Ocean; this justifies the idea of an ice sheet dynamics for both hemispheres, with possibly different timings (and periodicities). The close synchroneity between the long glacial interstadials observed in Greenland and Antarctica (as far as chronologies are accurate [*Bender et al.*, 1994]) can be explained by a global teleconnection, through the ocean circulation or eustatic sea level. It appears that isotopic fast variations at Vostok can be slightly in advance compared to those at GRIP/GISP2 [*Jouzel et al.*, 1996] . This suggests that the climate system during an ice age is able to contain (at least) two coupled oscillating subsystems located in both hemispheres [*Yiou et al.*, 1995].

The $\delta^{18}O$ residual, with respect to Ca content at GRIP, also has an intriguing behavior. By construction, it is not driven by local (high latitude) climate, like the isotopic or calcium records. Instead, it is dominated by a precessional component which indicates a low-latitude influence. It hence offers an alternative to deuterium excess [*Jouzel et al.*, this issue] to account for source variablity, and the connection between these two variables will be investigated further.

The Holocene shows significant quasi-periodic components between 100 and 200 years. This behavior is within the range of oceanic variability [*Stocker and Mysak*, 1992; *Mann et al.*, 1995] during this stable climatic stage and has been simulated with simplified

oceanic general circulation models [*Weaver et al.*, 1993; *Quon and Ghil*, 1995; *Rahmstorf*, 1995]. Another potential source of variability at this time scale comes from the solar forcing, at periodicities close to 208 and 80 years [*Stuiver et al.*, 1995]. At least, it testifies to a natural variability of the climatic system, even in a climate that appears to be stable to ice sheet/climate interactions.

In conclusion, we have detected general spectral characteristic features of the climatic system on three time scales and periods of the late Quaternary. Those oscillations are useful to constrain the time behavior of (coupled) climate models for long-term simulations. The next step will be to generalize this approach to a more extensive network of paleodata, as proposed by *Yiou et al.* [1994].

Appendix

The major difficulty with the MTM spectral estimates is the necessity of calculating the tapers. In general, extensive and complex calculations must be repeated for series of different length. The MEM and SSA approaches are limited in their application because of the need to keep the number of "lags" at a manageable level (which often requires subsampling as noted above). *Riedel and Sidorenko* [1995] propose "minimum bias tapers" which, for long series, can be taken as simple sine functions requiring no preliminary calculations, yield minimum bias estimates of spectral features, display, essentially, the same bandwidth as the tapers used in MTM [*Thomson*, 1982], and avoid the time-consuming computations which they require.

Traditional Fourier analysis assumes a stationary process, and, as noted above, this is not a reasonable assumption for most paleoclimate series. For such series the spectral estimates are really estimates of average "power" at a given frequency. One solution, as previously noted, is to perform separate analyses on discrete sections of a series in which the assumption of stationarity is not obviously invalid. This approach hinders the study of the long time scale components of the series and the processes involved in the transitions between approximately stationary segments. An alternative is to develop techniques which aid in interpreting how the "average power" at a Fourier frequency is distributed throughout the series.

One such technique is the SSA procedures previously discussed. Linear combinations of the selected eigenvectors (EOF components) represent the series component associated with the selected features of the spectrum. Two other methods based on digital filtering techniques are available. They have the advantage of not being limited in scope by the need to keep the embedding dimension, M, of the SSA approach to a manageable size. For that reason, both filtering methods can be used to explore both high- and low-frequency behavior in a uniformly sampled time series without the resampling which might be required by SSA.

Very efficient digital filters, low-pass, high-pass, and band-pass, can now be easily constructed [*Krause et al.*, 1993] and used to explore particular features of an estimated spectrum. The modulated sinusoidal output from a narrow band-pass filter describes how the energy in the passband is distributed in time throughout the series [*Mayewski et al.*, this issue; *Meeker et al.*, this issue]. Filters associated with different spectral peaks can be combined to form filter banks. The sum of the outputs from the filter bank is comparable to the reconstruction based on SSA [*Vautard et al.*, 1992]. In fact, extensive testing on synthetic series has shown that the reconstructions are, essentially, indistinguishable for short series or relatively high frequency behavior in long series where both methods can be used.

Such a filter bank must be designed and tested on synthetic series to insure its ability to estimate modulated sinusoids without distortion. Elliptic filters of orders 3 to 7 were utilized by [*Mayewski et al.*, this issue] and [*Meeker et al.*, this issue] to investigate spectral peaks at periodicities ranging from 1000 to 40,000 years. Because the filters of a filter bank are not perfect their passbands are not disjoint and the filter outputs are only approximately orthogonal. The filter outputs can be orthogonalized and used as a basis for a linear subspace of series having the selected spectral features. Projection of the original series on this subspace is analogous to the projection on the EOF subspace of SSA and yields a least squares approximating time series with the spectrum prescribed by the filter bank. Projection on each of the orthogonal basis vectors provides an analysis of the variance associated with each spectral peak [*Mayewski et al.*, this issue; *Meeker et al.*, this issue]. In each case the estimated almost periodic components (modulated sinusoids) should be compared with the ordinary periodic Fourier components obtained by projection on sinusoidal components of the same frequency in order to assess the significance of the modulation, small shifts in phase, and gain in variance explained. If a filter has been properly designed and tested on synthetic series for its ability to extract modulated sinusoids from a noisy background, the proportion of variance of the original series explained by its particular output component provides a direct assessment of the significance of the estimated spectral peak.

Complex demodulation is another filtering technique used to estimate modulated sinusoidal components from time series [*Bloomfield*, 1976]. Given a series with a spectral peak at an estimated frequency $\hat{f}$ and an assumed component

$$a_t \cos(2\pi \hat{f} t + \phi_t) = a_t \left(\frac{e^{i2\pi \hat{f} t + \phi_t} + e^{-i2\pi \hat{f} t - \phi_t}}{2} \right) \quad (A1)$$

with a_t and ϕ_t unknown, the series is multiplied by $\exp(-i2\pi \hat{f} t)$ to cancel the oscillatory behavior at that frequency in the first exponential and shift the other to the higher frequency $2\hat{f}$. The product series is then filtered with a low-pass filter to estimate the modulus and

phase of the oscillatory signal from the slowly varying output of the filter, $a_t \exp(i\phi_t)/2$. Again, complex demodulation and direct band-pass filtering yield results which are similar and agree with SSA for short series. The advantage of complex demodulation is in the direct estimate of amplitude, a_t, and phase, ϕ_t, of the modulated signal.

References

Allen, M., Interactions between the atmosphere and oceans on time scales of weeks to years, Ph.D. thesis, St. John's Coll., Oxford Univ., England, 1992.

Allen, M. R. and A. W. Robertson, Distinguishing modulated oscillations from coloured noise in multivariate datasets, *Clim. Dyn.*, *12*, 775–784, 1996.

Alley, R. B., R. C. Finkel, K. Nushizumi, S. Anandakrishnan, C. A. Shuman, and P. A. Mayewski, Changes in continental and seasalt atmospheric loadings in central Greenland during the most recent deglaciation: Model based estimates, *J. Glaciol.*, in press.

Barnola, J. M., D. Raynaud, Y. N. Korotkevitch, and C. Lorius, Vostok ice core provides 160,000-year record of atmospheric CO_2, *Nature*, *329*, 408–414, 1987.

Bender, M., T. Sowers, M. L. Dickson, J. Orchardo, P. Grootes, P. A. Mayewski, and D. Meeses, Climate correlations between Greenland and Antarctica during the past 100,000 years, *Nature*, *372*, 663–666, 1994.

Benoist, J. P., Analyse spectrale de signaux glaciologiques: Etude des glaces sédimentaires déposées à Dome C, morphologie du lit d'un glacier, Thèse d'Etat, Univ. Grenoble, France, 1986.

Berger, A. L., M. F. Loutre, and C. Tricot, Insolation and Earth's orbital periods, *J. Geophys. Res.*, *98*, 10,341–10,362, 1993.

Birchfield, G. E. and M. Ghil, Climate evolution in the Pliocene-Pleistocene as seen in deep sea $\delta^{18}O$ records and in simulations: Internal variability versus orbital forcing, *J. Geophys. Res.*, *98*, 10,385–10,399, 1993.

Bloomfield, P., *Fourier Analysis of Time Series: An Introduction*, John Wiley, New York, 1976.

Bond, G., W. S. Broecker, S. Johnsen, J. McManus, L. Labeyrie, J. Jouzel, and G. Bonani, Correlations between climate records from North Atlantic sediments and Greenland ice, *Nature*, *365*, 143–147, 1993.

Bond, G. C. and R. Lotti, Iceberg discharges into the North Atlantic on millenial time scales during the last deglaciation, *Science*, *267*, 1005–1010, 1995.

Broecker, W. S., G. Bond, M. Klas, E. Clark, and J. McManus, Origin of the northern Atlantic's Heinrich events, *Clim. Dyn.*, *6*, 265–273, 1992.

Broomhead, D. S. and G. P. King, Extracting qualitative dynamics from experimental data, *Physica D 20*, 217–236, 1986.

Burg, J. P., Maximum entropy spectral analysis, paper presented at the 37th Annual International Meeting, Soc. Explor. Geophys., Oklahoma City, Okla., 1967.

Chappellaz, J., J. M. Barnola, D. Raynaud, Y. S. Korotkevitch, and C. Lorius, Ice-core record of atmospheric methane over the past 160,000 years, *Nature*, *345*, 127–131, 1990.

Chappellaz, J., T. Blunier, D. Raynaud, J. M. Barnola, J. Schwander, and B. Stauffer, Synchronous changes in atmospheric CH_4 and Greenland climate between 40 and 8 kyr BP, *Nature*, *366*, 443–445, 1993.

Chappellaz, J., E. Brook, T. Blunier, and B. Malaizé, CH_4 and $\delta^{18}O$ of O_2 records from Antartic and Greenland ice: A clue for stratigraphic disturbance in the bottom of the Greenland Ice Core Project and the Greenland Ice Sheet Project 2 ice cores, *J. Geophys. Res.*, this issue.

Chen, F. and M. Ghil, Interdecadal variablity of the thermohaline circulation and high-latitude surface fluxes, *J. Phys. Oceanogr.*, *25*, 2547–2568, 1995.

Chen, F. and M. Ghil, Interdecadal variability in a hybrid coupled ocean-atmosphere model, *J. Phys. Oceanogr.*, *26*, 1561–1578, 1996.

Childers, D. G. (ed.), *Modern Spectrum Analysis*, IEEE Press, Piscataway, N. J., 1978.

Cortijo, E., P. Yiou, L. D. Labeyrie, and M. Cremer, Sedimentary record of climatic variability in the North Atlantic Ocean during the last glacial cycle, *Paleoceanography*, *10*, 911–926, 1995.

Crowley, T. J. and G. B. North, *Paleoclimatology*, Oxford Univ. Press, New York, 1991.

Cuffey, K. M., G. D. Clow, R. B. Alley, M. Stuiver, E. D. Waddington, and R. W. Saltus, Large Artic temperature change at the Wisconsin-Holocene glacial transition, *Science*, *270*, 455–458, 1995.

Dansgaard, W., et al., Evidence for general instability of past climate from a 250-kyr ice-core record, *Nature*, *364*, 218–220, 1993.

Delworth, T., S. Manabe, and R. Stouffer, Interdecadal variations of the thermohaline circulation in a coupled ocean-atmosphere model, *J. Clim.*, *6*, 1993–2011, 1993.

Dettinger, M. D., M. Ghil, C. M. Strong, W. Weibel, and P. Yiou, Software expedites singular-spectrum analysis of noisy time series, *Eos Trans. AGU*, *76*, 12, 20, 21, 1995.

Fuhrer, K., A. Neftel, M. Anklin, and V. Maggi, Continuous measurements of hydrogen peroxide, formaldehyde, calcium and ammonium concentrations along the new GRIP core from Summit, central Greenland, *Atmos. Environ. Sect. A*, *27*, 1873–1880, 1993.

Ghil, M. and S. Childress, *Topics in Geophysical Fluid Dynamics: Atmospheric Dynamics, Dynamo Theory and Climate Dynamics*, Springer-Verlag, New York, 1987.

Ghil, M. and H. Le Treut, A climate model with cryodynamics and geodynamics, *J. Geophys. Res.*, *86*, 5262–5270, 1981.

Ghil, M. and P. Yiou, Spectral methods: What they can and cannot do for climatic time series, in *Decadal Climate Variability: Dynamics and Predictability*, edited by D. Anderson and J. Willebrand, pp. 445–481, Elsevier, New York, 1996.

Ghil, M., A. Mullhaupt, and P. Pestiaux, Deep water formation and Quaternary glaciations, *Clim. Dyn.*, *2*, 1–10, 1987.

Ghil, M., M. Kimoto, and J. D. Neelin, Nonlinear dynamics and predictability in the atmospheric sciences, *U.S. Natl. Rep. Int. Union. Geod. Geophys.*, *1987–1990*, *Rev. Geophys.*, *27*, 46–55, 1991.

Grootes, P. M., M. Stuiver, J. W. C. White, S. Johnsen, and

J. Jouzel, Comparison of oxygen isotope records from the GISP2 and GRIP Greenland ice cores, *Nature*, *366*, 552–554, 1993.

Hagelberg, T. K., G. Bond, and P. deMenocal, Milankovitch band forcing of sub-Milankovitch climate variability during the Pleistocene, *Paleoceanography*, *9*, 545–558, 1994.

Haykin, S. and S. Kesler, Prediction-error filtering and maximum-entropy spectral estimation, in *Nonlinear Methods of Spectral Analysis, Top. Appl. Phys.*, vol. 34, edited by S. Haykin, pp. 9–72, Springer-Verlag, New York, 1983.

Hays, J. D., J. Imbrie, and N. J. Shackleton, Variations in the Earth's orbit: Pacemaker of the ice ages, *Science*, *194*, 1121–1132, 1976.

Heinrich, H., Origin and consequences of cyclic ice-rafting in the northeast Atlantic Ocean, during the past 130,000 yrs, *Quat. Res.*, *29*, 143–152, 1988.

Imbrie, J., et al., On the structure and origin of major glaciations cycles, 1, Linear responses to Milankovitch forcing, *Paleoceanography*, *7*, 701–738, 1992.

Jenkins, G. M. and D. G. Watts, *Spectral Analysis and its Applications*, Holden-Day, Merrifield, Va., 1968.

Johnsen, S. J., W. Dansgaard, and J. W. White, The origin of Arctic precipitation under present glacial conditions, *Tellus, Ser. B*, *41*, 452–468, 1989.

Johnsen, S. J., H. B. Clausen, W. Dansgaard, K. Fuhrer, N. Gundestrup, C. U. Hammer, P. Iversen, J. Jouzel, B. Stauffer, and J. P. Steffensen, Irregular glacial interstadials recorded in a new Greenland ice core, *Nature*, *359*, 311–313, 1992.

Johnsen, S. J., H. B. Clausen, W. Dansgaard, N. S. Gundestrup, C. U. Hammer, and H. Tauber, The Eem stable isotope record along the GRIP ice core and its interpretation, *Quat. Res.*, *43*, 117–124, 1995a.

Johnsen, S. J., D. Dahl-Jensen, W. Dansgaard, and N. S. Gundestrup, Greenland temperatures derived from the GRIP borehole temperature and ice isotope profiles, *Tellus, Ser. B*, *47*, 624–629, 1995b.

Jouzel, J., and L. Merlivat, Deuterium and oxygen 18 in precipitation: Modeling of the isotopic effects during snow formation, *J. Geophys. Res.*, *89*, 11,749–11,757, 1984.

Jouzel, J., C. Lorius, J. R. Petit, C. Genthon, N. I. Barkov, V. M. Kotlyakov, and V. M. Petrov, Vostok ice core: a continuous temperature record over the last climatic cycle (160,000 years), *Nature*, *329*, 403–408, 1987.

Jouzel, J., et al., Extending the Vostok ice-core records of palaeoclimate to the penultimate glacial period, *Nature*, *364*, 407–412, 1993.

Jouzel, J., R. D. Koster, R. J. Suozzo, and G. L. Russel, Stable water isotope behavior during the last glacial maximum: A general circulation model analysis, *J. Geophys. Res.*, *99*, 25,791–25,801, 1994.

Jouzel, J., C. Hammer, C. Lorius, S. Johnsen, P. Grootes, M. Stievenard, and J. White, Abrupt climate changes: A global perspective from ice cores, in *Clouds, Chemistry and Climate NATO ASI Ser. I, vol. 35*, edited by P. J. Crutzen and V. Ramanathan), pp. 83–108, Springer-Verlag, New York, 1996.

Jouzel, J., R. Alley, K. M. Cuffey, W. Dansgaard, P. Grootes, S. Johnsen, R. Koster, D. Peel, M. Stievenard, M. Stuiver, and J. White, Validity of the temperature reconstruction from water isotopes in ice cores, *J. Geophys. Res.*, this issue.

Krause, T. P., L. Shure, and J. N. Little, *Signal Processing Toolbox*, MathWorks, Natick, Mass., 1993.

Kutzbach, J. E. and P. J. Guetter, The sensitivity of monsoon climates to orbital parameter changes for 9000 years B.P.: Experiments with the NCAR general circulation model, in *Milankovitch and Climate* edited by A. Berger, et al., pp. 801–820, Norwell, Mass., 1984.

Kutzbach, J. E. and B. L. Otto-Bliesner, The sensitivity of the African-Asian monsoonal climate to orbital parameter changes for 9000 years B.P. in a low-resolution general circulation model, *J. Atmos. Sci.*, *39*, 1177–1188, 1982.

Lall, U. and M. Mann, The Great Salt Lake: A barometer of low-frequency climatic variability, *Water Resource Res.*, *31*, 2503–2515, 1995.

Legrand, M., M. DeAngelis, T. Stafflebach, A. Neftel, and B. Stauffer, Large perturbations of ammonium and organic acids content in the Summit-Greenland ice core. Fingerprint from forest fires?, *Geophys. Res. Lett.*, *19*, 473–475, 1992.

Legrand, M., M. DeAngelis, and F. Maupetit, Field investigation of major and minor ions along Summit (Central Greenland) ice core by ions chromatography, *J. Chromatogr.*, *460*, 251–258, 1993.

Lorius, C., J. Jouzel, C. Ritz, L. Merlivat, N. I. Barkov, V. M. Kotlyakov, and V. M. Petrov, A 150,000 year climatic record from Antarctic ice, *Nature*, *316*, 591–596, 1985.

MacAyeal, D. R., A low-order model of the Heinrich event cycle, *Paleoceanography*, *8*, 767–773, 1993.

Mann, M. E., J. Park, and R. S. Bradley, Global interdecadal and century-scale climate oscillations during the past five centuries, *Nature*, *378*, 266–270, 1995.

Marcus, S. L., M. Ghil, and J. O. Dickey, The extratropical 40-day oscillation in the UCLA general circulation model, I, Atmospheric angular momentum, *J. Atmos. Sci.*, *51*, 1431–1446, 1994.

Marcus, S. L., M. Ghil, and J. O. Dickey, The extratropical 40-day oscillation in the UCLA general circulation model, II, Spatial structure, *J. Atmos. Sci.*, *53*, 1993–2014, 1996.

Martinson, D. G., N. G. Pisias, J. D. Hays, J. Imbrie, T. C. Moore, and N. J. Shackleton, Age dating and the orbital theory of the ice ages: Development of a high-resolution 0 to 300,000-year chronostratigraphy, *Quat. Res.*, *27*, 1–30, 1987.

Mayewski, P. A., W. B. Lyons, M. J. Spencer, M. S. Twickler, C. F. Buck, and S. Whitlow, Recent increase in nitrate concentration of Antarctic snow, *Nature*, *346*, 554–556, 1990a.

Mayewski, P. A., M. J. Spencer, M. S. Twickler, and S. Whitlow, A glaciochemical survey of the Summit region, *Ann. Glaciol.*, *14*, 863–869, 1990b.

Mayewski, P. A., L. D. Meeker, M. C. Morrison, M. S. Twickler, S. Whitlow, K. K. Ferland, D. A. Meese, M. R. Legrand, and J. P. Stephenson, Greenland ice core "signal" characteristics: An expanded view of climate change, *J. Geophys. Res.*, *98*, 12,839–12,847, 1993a.

Mayewski, P. A., L. D. Meeker, S. Whitlow, M. S. Twickler, M. C. Morrison, R. B. Alley, P. Bloomfield, and K. Taylor, The atmosphere during the Younger Dryas, *Science*, *261*, 195–197, 1993b.

Mayewski, P. A., et al., Changes in atmospheric circulation and ocean ice cover over the North Atlantic during the last 41,000 years, *Science*, *263*, 1747–1751, 1994.

Mayewski, P. A., L. D. Meeker, M. S. Twickler, S. I. Whitlow, Q. Yang, and M. Prentice, Major features and forcing of high latitude northern hemispheric atmospheric circulation using a 110,000-year-long glaciochemical series, *J. Geophys. Res.*, this issue.

Meeker, L. D., P. A. Mayewski, M. S. Twickler, S. I. Whitlow, and D. Meese, A 110,000-year history of change in continental biogenic emissions and related atmospheric circulation inferred from the Greenland Ice Sheet Project 2 ice core, *J. Geophys. Res.*, this issue.

Meese, D., A. Gow, R. B. Alley, P. M. Grootes, G. A. Zielinski, M. Ram, K. C.Taylor, P. Mayewski, and J. F. Bolzan, The Greenland Ice Sheet Project 2 depth-age scale: Methods and results, *J. Geophys. Res.*, this issue.

O'Brien, S. R., P. A. Mayewski, L. D. Meeker, D. A. Meese, M. S. Twickler, and S. I. Whitlow, Complexity of Holocene climate as reconstructed from a Greenland ice core, Science, 270, 1962-1964, 1996.

Packard, N. H., J. P. Crutchfield, J. D. Farmer, and R. S. Shaw, Geometry from a time series, Phys. Rev. Lett., 45, 712-716, 1980.

Paillard, D. and L. D. Labeyrie, Role of the thermohaline circulation in the abrupt warming after Heinrich events, Nature, 372, 162-164, 1994.

Peixoto, J. P. and A. H. Oort, Physics of Climate, Am. Inst. Phys., New York, 1992.

Penland, C., M. Ghil, and K. Weickmann, Adaptive filtering and maximum entropy spectra, with application to changes in atmospheric angular momentum, J. Geophys. Res., 96, 22,659-22,671, 1991.

Percival, D. B. and A. T. Walden, Spectral Analysis for Physical Applications, Cambridge Univ. Press, New York, 1993.

Petit, J. R., L. Mounier, J. Jouzel, Y. S. Korotkevitch, V. I. Kotlyakov, and C. Lorius, Paleoclimatological and chronological implications of the Vostok dust record, Nature, 343, 56-58, 1990.

Plaut, G. and R. Vautard, Spells of low-frequency oscillations and weather regimes in the northern hemisphere, J. Atmos. Sci., 51, 210-236, 1994.

Preisendorfer, R. W., Principal Component Analysis in Meteorology and Oceanography, Elsevier, New York, 1988.

Quon, C. and M. Ghil, Multiple equilibria and stable oscillations in thermosolutal convection at small aspect ratio, J. Fluid Mech., 291, 33-56, 1995.

Rahmstorf, S., Bifurcation of the Atlantic thermohaline circulation in response to changes in the hydrological cycle, Nature, 378, 145-149, 1995.

Riedel, K. S. and A. Sidorenko, Minimum bias multiple taper spectral estimation, IEEE Trans. Signal Process., 43, 188-195, 1995.

Rögnvaldsson, Ö. E., Spectral estimation using the multitaper method, Tech. Rep. RH-13-13, Sci. Inst., Univ. of Iceland, Reykjavik, 1993.

Shemesh, A., L. H. Burckle, and J. D. Hays, Meltwater input to the Southern Ocean during the last glacial maximum, Science, 266, 1542-1544, 1994.

Sowers, T., M. Bender, L. D. Labeyrie, D. Martinson, J. Jouzel, D. Raynaud, J. J. Pichon, and Y. S. Korotkevitch, A 135,000-year Vostok-SPECMAP common temporal framework, Paleoceanography, 8, 737-766, 1993.

Stocker, T. F. and L. A. Mysak, Climatic fluctuations on the century time-scale: a review of high-resolution proxy data and possible mechanisms, Clim. Change, 20, 227-250, 1992.

Stuiver, M., P. M. Grootes, and T. F. Braziunas, The GISP2 $\delta^{18}O$ climate record of the past 16500 years and the sun, ocean, and volcanoes, Quat. Res., 44, 341-354, 1995.

Takens, F., Detecting strange attractors in turbulence, in Dynamical Systems and Turbulence, Lect. Notes Math., vol. 898, edited by D. A. Rand and L.-S. Young, pp. 366-381, Springer-Verlag, New York, 1981.

Taylor, K. C., C. U. Hammer, R. B. Alley, H. B. Clausen, D. Dahl-Jensen, A. J. Gow, N. S. Gundestrup, J. Kipfstuhl, J. C. Moore, and E. D. Waddington, Electrical conductivity measurements from the GISP2 and GRIP Greenland ice cores, Nature, 366, 549-552, 1993.

Thomson, D. J., Spectrum estimation and harmonic analysis, Proc. IEEE, 70, 1055-1096, 1982.

Thomson, D. J., Quadratic-inverse spectrum estimates: applications to palaeoclimatology, Phil. Trans. R. Soc. Lond. A, 332, 539-597, 1990.

Vautard, R. and M. Ghil, Singular spectrum analysis in nonlinear dynamics, with applications to paleoclimatic time series, Physica D 35, 395-424, 1989.

Vautard, R., P. Yiou, and M. Ghil, Singular spectrum analysis: a toolkit for short noisy chaotic signals, Physica D 58, 95-126, 1992.

Verbitsky, M. Y. and B. Saltzman, Heinrich-type glacial surges in a low-order dynamical climate model, Clim. Dyn., 10, 39-47, 1994.

Verbitsky, M. Y. and B. Saltzman, A diagnostic analysis of Heinrich glacial surge events, Paleoceanography, 1, 59-65, 1995.

Vostok Project Members, International effort helps decipher mysteries of paleoclimate from Antarctic ice cores, Eos Trans. AGU, 76, 169, 1995.

Waelbroeck, C., J. Jouzel, L. D. Labeyrie, C. Lorius, M. Labracherie, M. Stiévenard, and N. I. Barkov, Comparing the Vostok ice deuterium record and series from Southern Ocean core MD88-770 over the last two glacial-interglacial cycles, Clim. Dyn., 12, 113-123, 1995.

Weaver, A. J. and T. M. C. Hughes, Rapid interglacial climate fluctuations driven by North Atlantic ocean circulation, Nature, 367, 447-450, 1994.

Weaver, A. J., J. Marotzke, P. F. Cummins, and E. S. Sarachik, Stability and variability of the thermohaline circulation, J. Phys. Oceanogr., 23, 39-60, 1993.

Yang, J. and D. J. Neelin, Sea-ice interaction with the thermohaline circulation, Geophys. Res. Lett., 20, 217, 1993.

Yiou, P., C. Genthon, J. Jouzel, M. Ghil, H. Le Treut, J. M. Barnola, C. Lorius, and Y. N. Korotkevitch, High-frequency paleovariability in climate and in CO_2 levels from Vostok ice-core records, J. Geophys. Res., 96, 20,365-20,378, 1991.

Yiou, P., M. Ghil, J. Jouzel, D. Paillard, and R. Vautard, Nonlinear variability of the climatic system, from singular and power spectra of Late Quaternary records, Clim. Dyn., 9, 371-389, 1994.

Yiou, P., J. Jouzel, S. Johnsen, and Ö. E. Rögnvaldsson, Rapid oscillations in Vostok and GRIP ice cores, Geophys. Res. Lett., 22, 2179-2182, 1995.

Yiou, P., M. F. Loutre, and E. Baert, Spectral analysis of climate data, Surv. Geophys., 17, 619-663, 1996.

K. Fuhrer, Physikalisches Institut, Universität Bern, Sidlerstrasse 5, 3012 Bern, Switzerland.

S. Johnsen, Geophysical Institute, University of Copenhagen, Haraldsgade 6, 2200 N, Copenhagen, Denmark; Science Institute, University of Reykjavik, Dunhaga 3, Reykjavik 107, Iceland.

J. Jouzel and P. Yiou, Laboratoire de Modélisation du Climat et de l'Environnement, Commissariat à l'Energie Atomique, Direction des Sciences de la Matière, CE Saclay, l'Orme des Merisiers, 91191 Gif-sur-Yvette, France. (email: pyiou@cea.fr)

P. A. Mayewski and L. D. Meeker, Glacier Research Group and Climate Change Research Center, Institute for the Study of Earth, Ocean and Space, University of New Hampshire, Durham, NH 03824, USA.